

Article

Application and Practice of Variable Axial Force Cable in Powerhouse Truss Reinforcement System

Zizhen Shen ^{1,*}, Min Hong ², Xunfeng Li ¹, Zigang Shen ³, Lianbo Wang ^{4,*} and Xueping Wang ¹¹ School of Architectural Engineering, Zhejiang College of Construction, Hangzhou 310053, China² School of Materials Science and Engineering, Shanghai Jiao Tong University, Shanghai 200240, China³ Zhejiang Min An Testing Technology Co., Hangzhou 310000, China⁴ School of Materials Science and Engineering, Shanghai Institute of Technology, Shanghai 201418, China

* Correspondence: hzhgjc123@126.com (Z.S.); lbwabg@sit.edu.cn (L.W.)

Abstract: Long-span steel structure trusses are widely used in factory buildings. However, with the increase in service time and dynamic load fatigue, transverse cracks at the bottom of the middle span and oblique deformation of the abdomen during the operation process may appear in a considerable part of long-span trusses with dynamic load. The U-shaped cracks at the bottom and belly, as well as the mid-span down deflection of the main truss, can also reduce the functionality of the factory building truss structure and limit the original crane load, thus affecting the normal safety and durability of the structure. Therefore, the principle of variable axial force cable system in the long-span factory building truss structure and 3D3S software modelling were applied. Analysing and studying the reinforcement method of large-span powerhouse trusses can provide practical experience for subsequent similar projects. In view of the above phenomenon, the large-span powerhouse trusses of Hongcheng Powerhouse No. 1 and No. 2, located in Tonglu, Zhejiang Province, were used as the research objects, and the variable axial force cable method was proposed to strengthen and lift the load. Considering the span of the powerhouse truss, a cable system with 22 m and a controlling force of 400 kN was proposed for Powerhouse 1, and a cable system with a variable axial force of 24 m was proposed for Powerhouse 2. The force model of large-span trusses was established by using the finite element method, which is commonly used to analyse the force of the truss. The influence of the reinforcement effect was analysed under two working conditions and compared from three aspects: stiffness, bearing capacity and stability. Furthermore, the phenomenon of uneven stress distribution was analysed. The stress distribution characteristics of each node were understood by simulating the most disadvantageous node plates with the greatest internal force before and after reinforcement.

Keywords: long-span steel structure truss; variable axial force cable; 3D3S finite element model; joint plate analysis; variable system reinforcement combination stiffness; load domain



Citation: Shen, Z.; Hong, M.; Li, X.; Shen, Z.; Wang, L.; Wang, X.

Application and Practice of Variable Axial Force Cable in Powerhouse Truss Reinforcement System.

Buildings **2023**, *13*, 1271. <https://doi.org/10.3390/buildings13051271>

Academic Editor: Hiroshi Tagawa

Received: 21 March 2023

Revised: 27 April 2023

Accepted: 29 April 2023

Published: 12 May 2023



Copyright: © 2023 by the authors. Licensee MDPI, Basel, Switzerland. This article is an open access article distributed under the terms and conditions of the Creative Commons Attribution (CC BY) license (<https://creativecommons.org/licenses/by/4.0/>).

1. Introduction

Many previous researchers have conducted corresponding research on the application of variable axial force cables in reinforcement engineering. For example, the application of variable axial force cables in bridge reinforcement has been widely studied. One study investigated the application of VLM.TS-type outer cable in the Dongming Huanghe Bridge reinforcement project [1]. Gong proposed strengthening the Pu Shan Wan cantilever bridge using a cable system [2]. Hu et al. studied the application of 2000 MPa parallel steel cables in highway and cable bridges [3]. Simultaneously, the application of the variable axial force cable in bridge reinforcement has attracted the attention of researchers [4]. For example, He et al. conducted a stress and reinforcement analysis of steel truss structures considering the influence of global joint stiffness [5]. Pan studied the application of cable installation and construction technology of single-tower suspension bridges [6]. Yu et al. studied the application of cable installation and construction technology of composite beam suspension bridges.

The Variable Axial Load Cable Method is a structural retrofitting technique used to strengthen trusses. This method involves the installation of steel cables with appropriate tension to transfer the loads from weak or damaged members of the truss to stronger ones.

The process of retrofitting through this method starts with the identification of the damaged or weak member(s) and an assessment of the truss system's overall strength. Once identified, steel cables are installed in place of the damaged or weakened member(s), so that the original load-bearing function is restored.

The cables are then pre-tensioned to a specified load and attached to the adjacent members of the truss. The tension in the cables is adjusted to ensure the load is evenly distributed among all members of the truss. This ensures that the strength of the entire truss system is improved without overloading any one member [7].

Additionally, a number of researchers have studied the application of variable axial force cables in concrete bridge reinforcement. For instance, Hu studied damage inversion analysis and variable system reinforcement of concrete bridges based on an equivalent sandwich beam model [8], whilst Zhao et al. applied and investigated the effect of a cable shock absorber in the Jiayu Yangtze River Highway Bridge [9]. Several studies have also cited the variable axial force cable construction and related technologies of the standard specification, such as building structure load calculation code (GB50009-2019) [10], steel structure construction quality acceptance code (GB50205-2014) [11], cable construction technical code (JGJ257-2012) [12] and building structure test technical code (GB/T50344-2019) [13]. Teng et al. determined the axial force on stay cables whilst accounting for their bending stiffness and rotational end restraints by free vibration test [14]. Other researchers have introduced the design method for the overall strength and stability of steel structures [15–18] and used advanced structural inspection and evaluation techniques, such as 3D3S modelling inspection [19–21], and introduced the stress loss and strength failure detection methods of some high-strength bolts and steel [22–24].

Finally, researchers have also used the variable axial force cable application in structural engineering experimental research and finite element (FE) analysis. For example, one study verified the FE analysis method by conducting experiments on reinforced concrete beams [25], whilst another study conducted the stiffness evaluation and FE analysis of fibre-reinforced epoxy resin laminates [26]. In summary, the variable axial force cable has been widely used in reinforcement engineering, with great success. In practical engineering, the construction scheme of the cable with variable axial force should be reasonably designed in accordance with the application research of the cable with variable axial force in reinforcement engineering and relevant standards, combined with the actual situation, thus improving the reinforcement effect. However, studies on the application of the variable axial force cable in reinforcement engineering of steel truss structures have been limited, thereby motivating this research.

As typical representatives of modern industrial buildings, large-span factory buildings have various structural forms, huge spans and weak seismic ability and can easily be affected by natural disasters and human factors. Therefore, how to improve the earthquake resistance and overall stability of large-span plants has always been a concern of researchers. Recently, variable axial force cable technology has gradually been widely used, as it can effectively resist the impact of earthquakes, wind and other abnormal loads; improve the structural stability and seismic ability of long-span factory buildings; and can be widely used in large bridges, high-rise buildings and other fields.

This paper explores the application of cable technology with variable axial forces in the reinforcement of large-span powerhouses. Taking two large-span powerhouses as examples, the influence of cable reinforcement with variable axial force on large-span powerhouse structure is studied through FE analysis and experimental verification. The results of this study can provide a theoretical and practical basis for seismic reinforcement of large-span powerhouses. Simultaneously, this paper also discusses the application prospects and development trends of the variable axial force cable reinforcement technology in other fields. Through this study, we make an important contribution to the structural

reinforcement and seismic capacity improvement of large-span factory buildings, as well as provide a useful reference for the sustainable development of modern industrial buildings.

2. Project Profile

Powerhouses 1 and 2 of Zhejiang Hongcheng Industrial Co., Ltd. are double-span gantry rigid steel structures. Industrial Powerhouse 1 was built in 2008, covering a building area of 11,200.3 m² and with an eaves elevation of 11.400 m, according to the fire risk classification D, fire resistance grade 2 and the redesigned safety grade 2. Powerhouse 1 has waterproof-grade III roofing and uses a moulding steel plate for defensive protection. As for the seismic fortification of this project category C, its seismic fortification intensity is 6°, the design basic acceleration is 0.05 g, and the engineering design life of the steel frame main body is good for 50 years.

Powerhouse 2 was also built in 2008, covering a building area of 5952 m² and with an eaves elevation of 11.100 m (slightly higher than Powerhouse 1). Its fire risk classification, fire resistance grade, safety grade, waterproof grade, seismic fortification category, seismic fortification intensity, design basic acceleration and engineering design life are the same as those of Powerhouse 1. The photos of the two house trusses are shown in Figures 1 and 2, respectively, whilst the corresponding section views of Powerhouses 1 and 2 are shown in Figures 3 and 4.



Figure 1. Powerhouse 1.



Figure 2. Powerhouse 2.

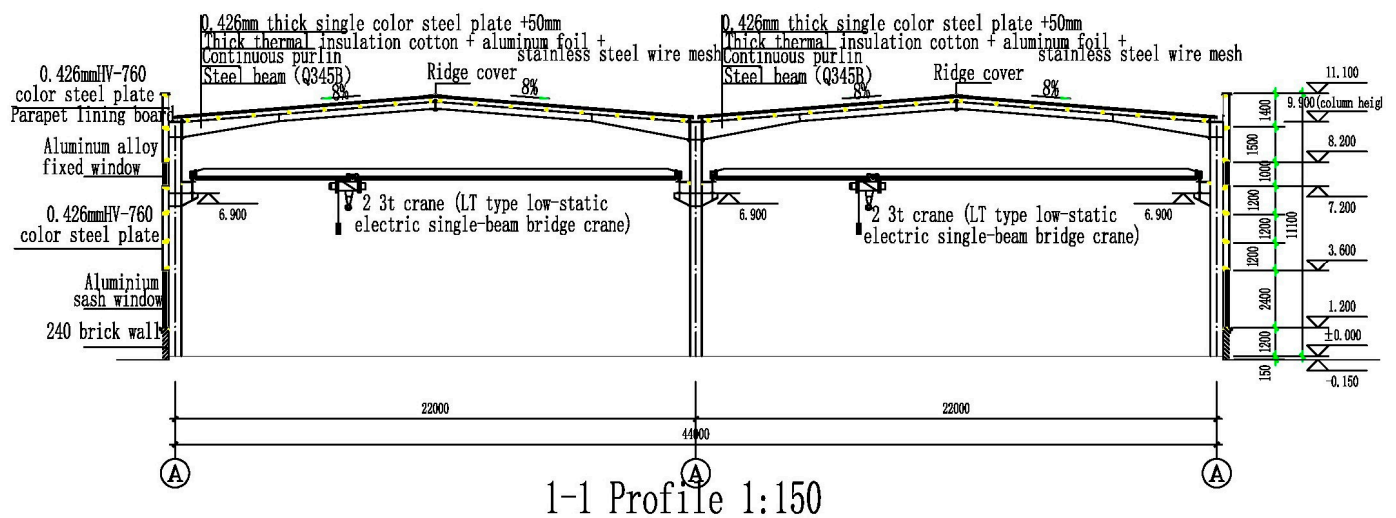


Figure 3. Cross-section view of Powerhouse 2.

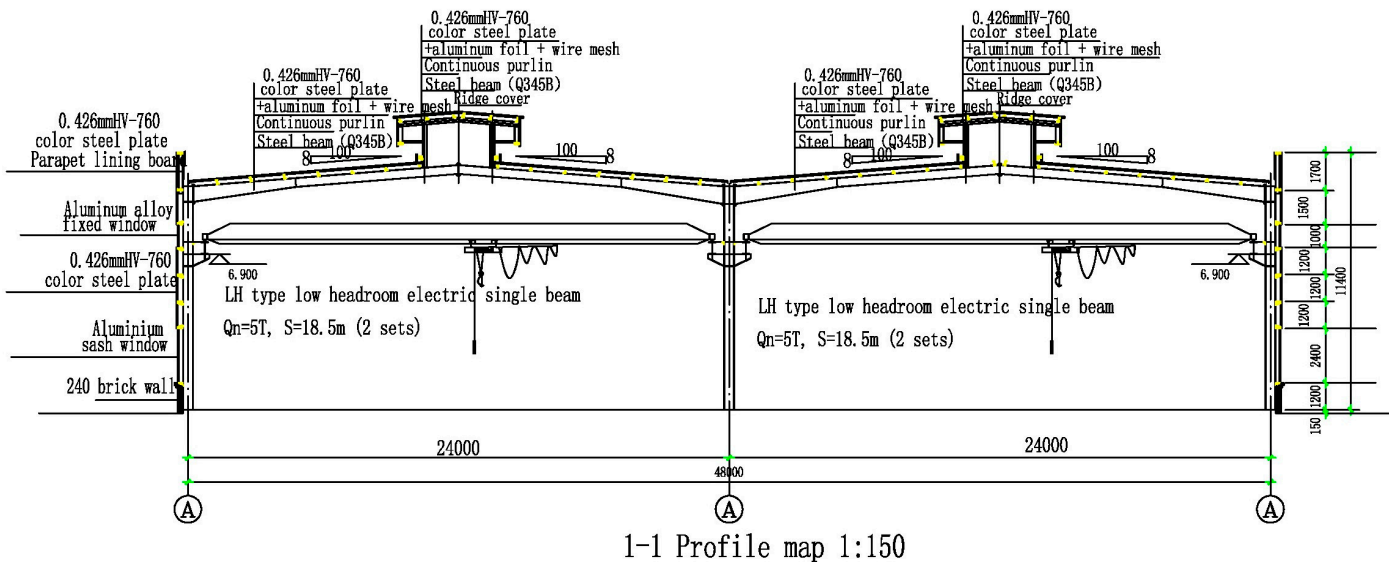


Figure 4. Cross-section view of Powerhouse 1.

3. Reinforcing Analysis

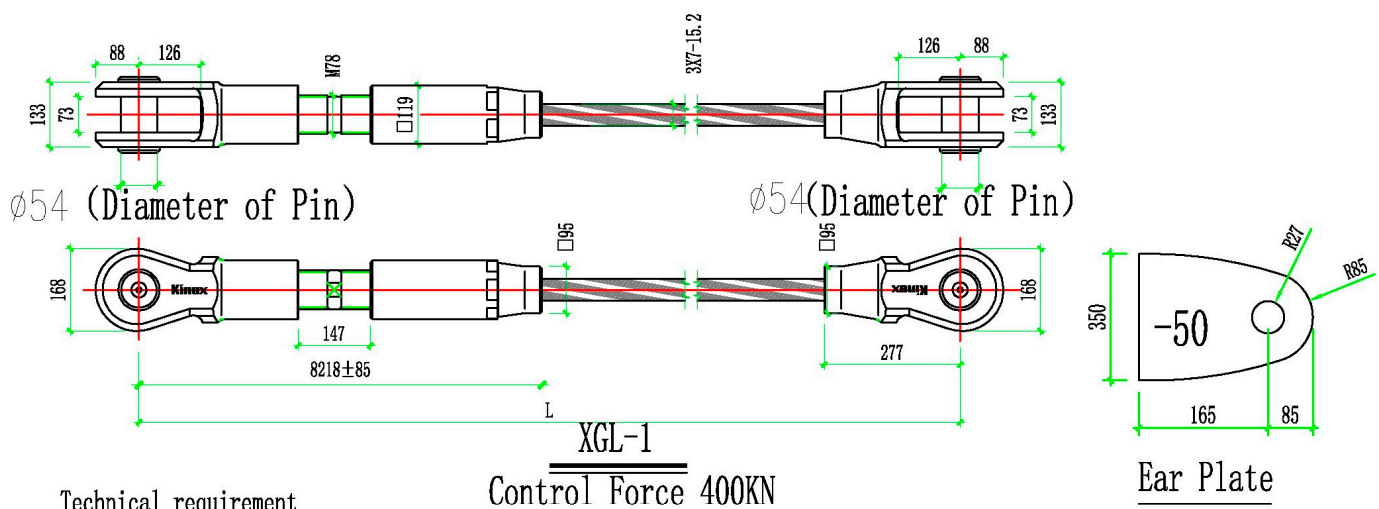
3.1. Reinforcement Scheme

Due to the addition of roof photovoltaic panels in the two plant buildings, the existing plant buildings cannot meet the requirements of the new code. Therefore, under the influence of the above two factors, the buildings must be strengthened comprehensively. Simultaneously, the roofs of the two factory buildings are cracked, causing water leakage that affects their normal use. Furthermore, the deflection of the truss exceeds the limit, the crane track is seriously worn, and the crane in the lane cannot pass normally. The plant area is reinforced and reformed under the influence of the new regulations.

Due to the large span of the trusses in the powerhouses of Zhejiang Hong Cheng Company, if the conventional increase force surface of the column is arranged between the rigid trusses, the headroom area of the powerhouse will be reduced, and the crane and the vehicles inside the powerhouse cannot be used or passed normally. Therefore, we selected a variable axial force cable for the overall truss reinforcement. The cable is arranged in a radial manner, and the anchor block is arranged in the purlin of the original rigid frame node. Upon reinforcement, the original truss only must bear the dead weight of the truss, whilst the new cable variable axial force bears two parts of the load, mainly

the dead weight and tension of the cable, as well as the additional dead load and other live loads of the truss, thereby improving the overall bearing capacity of the truss.

To summarise the prestressing force value of the cable, two kinds of cable calculations and comparisons were selected in this paper. Type 1 simulates the cable reinforcement with a low controlling force. The span of the original truss was 22 m, whilst the controlling force was 400 kN. For the cable reinforcement of the conventional control force in the Type 2 simulation, the span of the original truss was 24 m, and the control force was 600 kN, as shown in Figures 5 and 6. Through theoretical calculations and analysis, we obtained the influence of two kinds of cable reinforcement effects, from which information the whole node plates are designed.



Technical requirement

1. Steel cable adopts steel strand.
2. Steel wire resistance and tensile strength grade is 1860MPa.
3. Theoretical minimum breaking force of cable body is 781kN, and static load of cable is 100KN.
4. Cable making error: $\pm 15\text{mm}$.
5. Adjustable cable head, adjustable anchor cup, fixed cable head outer surface hot spray zinc after spraying zinc rich primer, pin shaft, pin cover plate, screw surface galvanized. After completion of construction, the construction unit will paint the anchorage of the cable twice, the same as the steel structure.

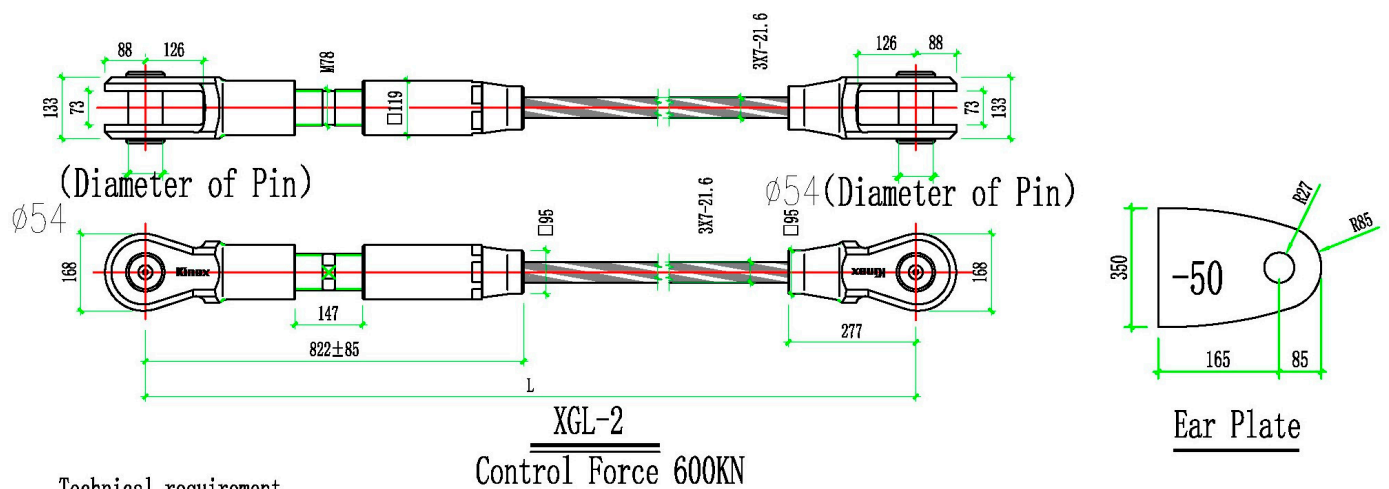
Figure 5. Detailed drawing of the variable axial force cable in Powerhouse 1.

3.2. Reinforcement Mechanism

In this study, we developed a method of cable reinforcement with variable axial force from a bridge system. The cable is a kind of cable-bearing bridge, in which the force form of the main truss is similar to the continuous beam that is supported by an elastic multi-point position. In truss calculations, the position and controlling force of the cable have a great influence on the whole force of the truss.

The main impact of changing the controlling force and position of the cable is that the height of the cable directly affects the dip angle of the cable. In the general truss design, the cable provides elastic support for the roof structure [1]. Therefore, to obtain a larger vertical component, a cable with a larger dip angle must be selected. A study of the bridge systems found that the ratio between the layout height of the conventional cable and the span of the truss generally ranges from 1/4–1/6, which is the reasonable layout height of a cable. If the height of the truss is short, the ratio between the layout height and the path of the truss generally ranges from 1/8–1/12 [2]. Due to the different layout heights, the stress characteristics of the two are also different. Simultaneously, for the transverse diameter cable tie truss/cover, both ends of the suspension cable can be designed to be equal or unequal height, and the sag should have a range of 1/10–1/20 of the span, according to JGJ257-2012 cable structure technical regulations [3]. Here, we selected the design value of

the cable control force and verified that this is actual practice, according to Articles 5.6.1 and 5.6.2 of the JGJ257-2012 Cable Structure Technical Regulations.



Technical requirement

1. Steel cable adopts steel strand.
2. Steel wire resistance and tensile strength grade is 1860MPa.
3. Theoretical minimum breaking force of cable body is 1590kN, and static load of cable is 100kN.
4. Cable making error: $\pm 15\text{mm}$.
5. Adjustable cable head, adjustable anchor cup, fixed cable head outer surface hot spray zinc after spraying zinc rich primer, pin shaft, pin cover plate, screw surface galvanized. After completion of construction, the construction unit will paint the anchorage of the cable twice, the same as the steel structure.

Figure 6. Detailed drawing of the variable axial force cable in Powerhouse 2.

3.3. Computational Analysis and Modelling

- (1) The overall situation is shown in Figures 3 and 4.
- (2) The force analysis of the 3/A axis column and the deformation analysis of the column section after stress are shown in Figure 7. The schematic diagram of the roof truss load G1 and crane beam load G2 is shown in Figure 8.

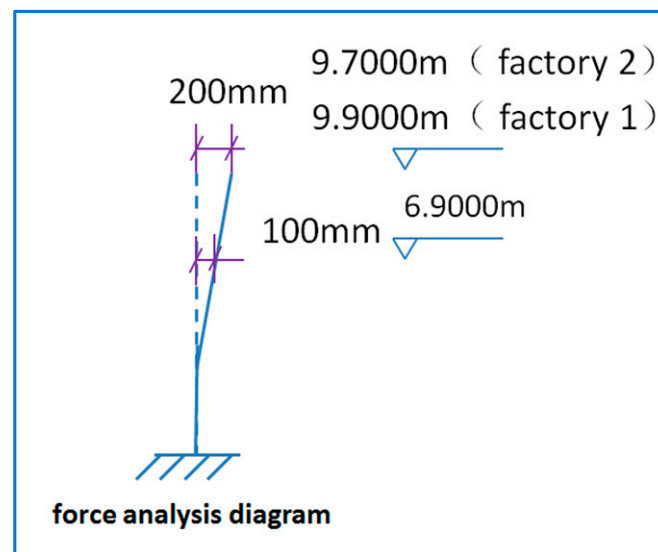


Figure 7. Column stress deformation diagram.

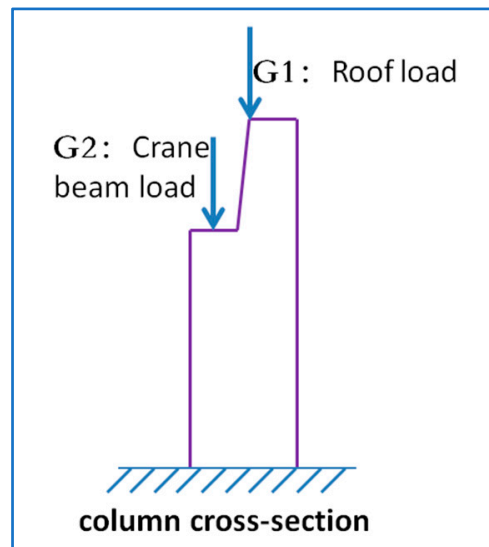


Figure 8. Column cross-section.

- (3) Analysis of the upper part: The height of the column section is within the height range of 16.9–9.9 m. The original eccentricity of G1 is 400 mm, which has turned 100 mm to the right—a condition that is favourable to the upper end and ensures that no breakage occurs. The calculation is based on the GB 50009-2019 building structure loading code.
- (4) Overall analysis (see Figure 9):

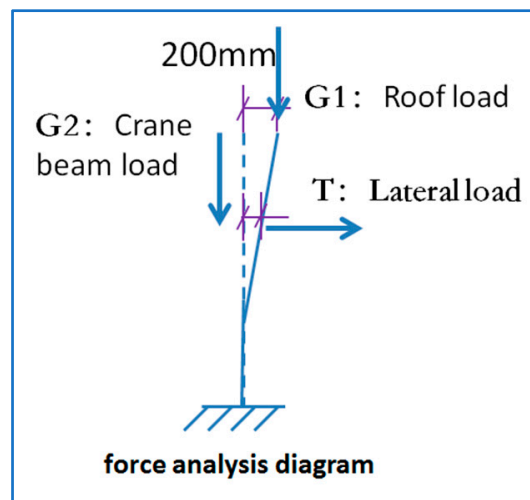


Figure 9. Schematic of the overall mechanical analysis.

G1: Original eccentricity + 0.3 (positive to the left)

G2: original eccentricity − 0.5

Deflection due to the column force:

G1: original eccentricity $e_1 = + 0.5$

G2: eccentricity becomes $e_2 = -0.4$

Based on the calculation of a single piece of house truss in Powerhouse 1:

- 1) Roof plate dead load: 3 kN/m^2 ; Live load: 0.5 kN/m^2 ; The span ranges from 22–24 m, with Seta pin spacing of 8 m

$$G_1 = (1.3 \times 3 + 1.5 \times 0.5) \times 8 \times 14 \times \frac{1}{2} = 45.9 \text{ kN}$$

- 2) Wind load: Using simplified calculation, we take 1 as a uniform load, and then the line load is as follows: $1 \times 8 = 8 \frac{\text{kN}}{\text{m}} = q_w$.
- 3) Vertical crane load (see Figure 10), because the eccentricity of the crane load is negative, the worst case is 0.

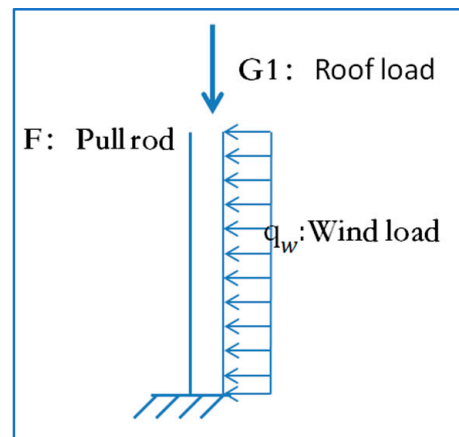


Figure 10. Schematic of vertical crane load mechanics.

- 4) Dead weight of the wall: $M_4 = 8 \times 0.3 \times 30 \times 22 \times 0.1 \times 1.3 = 205.4 \text{ kN/m}$
- 5) The horizontal load (transverse) of the crane is two sets of $Q = 20/5 \text{ t}$ soft hook crane A6 and heavy car.

$$\sum T_k = 2 \times 2 \times 0.1 \times \frac{5 + 20}{4} \times 9.8 = 24.5 \text{ kN}$$

$$M = M_1 + M_2 + M_4 + 0.7 \times M_5$$

For the convenience of calculation, we considered the roof live load, according to the dead load, to meet the guaranteed rate. This includes the following:

$$= 45.9 \times 0.5 + 205.4 + \frac{1}{2} \times 8 \times 30 \times 30 \times 1.5 + 0.7 \times 915.08 = 6268.906 \text{ kN/m}$$

- 6) Current situation: mm column bending capacity configuration: 10 HRB400 rebar with a diameter of 25 mm:

$$M_{\text{configuration}} = 2425 \text{ kN/m}$$

- 7) Horizontal tie-bar tension:

$$T = \frac{M}{11.4} = 549.9 \text{ kN}$$

When the current mm can bear part of the bending distance, then:

$$T = \frac{6268.906 - 2425}{11.4} = 337.18 \text{ kN}$$

We considered adding a cable rod between the columns at an elevation of 6.9 m. The cable rod coordinates the bending distance between the two ends [27]. It can either be removed after reinforcement or retained permanently (more suitable) to reduce the eccentricity of the columns.

- (5) 3D3S modelling was applied after importing the overall calculation data [28], as shown in Figures 11 and 12.

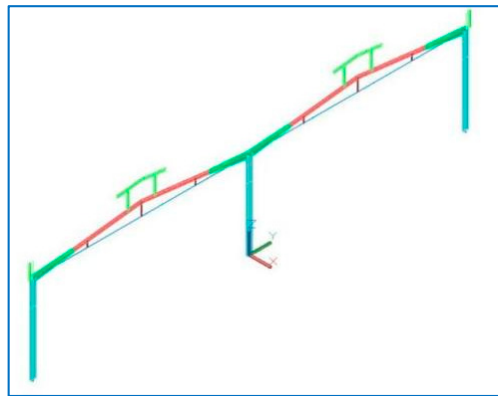


Figure 11. 3D3S model of the southeast axis.

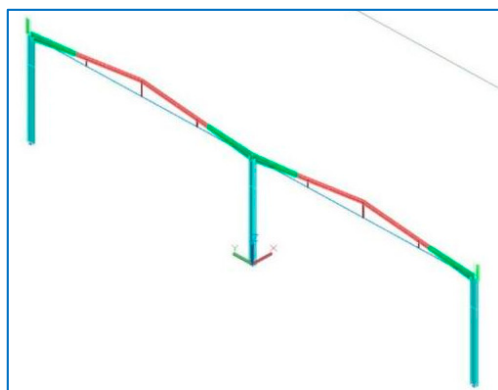


Figure 12. 3D3S model of the southwest axis.

3.3.1. Condition 1: Uniform Load

We compared and analysed the deflection values of different span trusses before and after reinforcement under a uniform load in working condition 1, as shown in Figure 11. The maximum deflection value was 55.42 mm before reinforcement, whilst the maximum deflection value was 12.52 mm after the span of 22 m. Compared with the state before reinforcement, the deflection value of each component decreased by more than 77.4%. The maximum deflection value of the cable span after reinforcement at 24 m was 15.64 mm. Compared with the state before reinforcement, the deflection value of each component decreased by more than 71.8% [29], as shown in Figure 13.

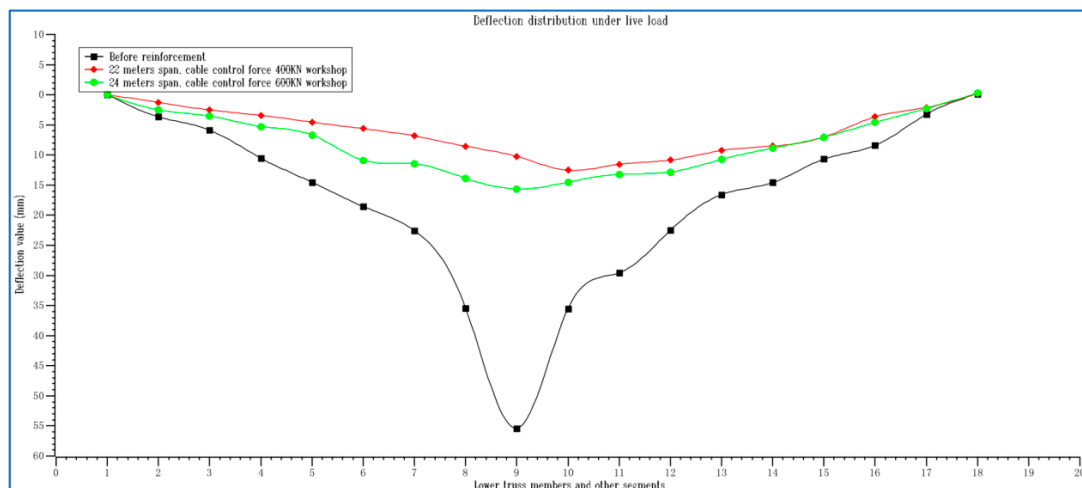


Figure 13. Deflection distribution under live load.

The difference in cable span and axial force led to a change in the cable dip angle. When the span and axial force of the cable changed, the components of the cable force along the X axis and the Z axis also differed, in which the larger the span, the larger the axial force (i.e., the larger the component along the Z axis, the larger the deflection reduction value). Compared with the axial forces of 400 kN with a 22 m span and 600 kN with a 24 m span, the reduction rate of the deflection value of the component strengthened with the latter was greater than that of the former under the same uniform load conditions. When the controlling force exceeded 600 kN, the reduction rate of the deflection value became smaller [30].

3.3.2. Condition 2: Stress Value

Table 1 lists the changes in the maximum stress value of the lower member after cable reinforcement. Combined with the data in the table and the stress distribution trend of the lower member of the truss in Figure 14, it can be seen that the stress system of the original truss changed after reinforcement, after which the internal forces of each truss member changed accordingly. Before the original truss reinforcement, it can be regarded as a simply supported truss structure, with the maximum bending moment value at the mid-span. The reinforced cable was similar to the elastic support, which changed the type of original structure, i.e., the 1-span 22 m/24 m truss changed into a 4-span 5.5 m/6 m continuous beam. Furthermore, the structural type and single span changed, greatly reducing the internal force value of the reinforced truss. After reinforcement, the initial tension of the cable expanded the range of the compression member of the truss under the action of dead load, whilst the tensile stress of the tension rod decreased.

Table 1. Changes in the stress values of lower truss members after cable reinforcement.

Span (m)/Control Force (kN)	Maximum Stress (MPa)	Stress Reduction (MPa)	Reduction Rate (%)
Before reinforcement	310.82	0.0	0.0
22 m/400 kN	112.52	212.54	65.38
24 m/600 kN	70.54	244.70	77.62

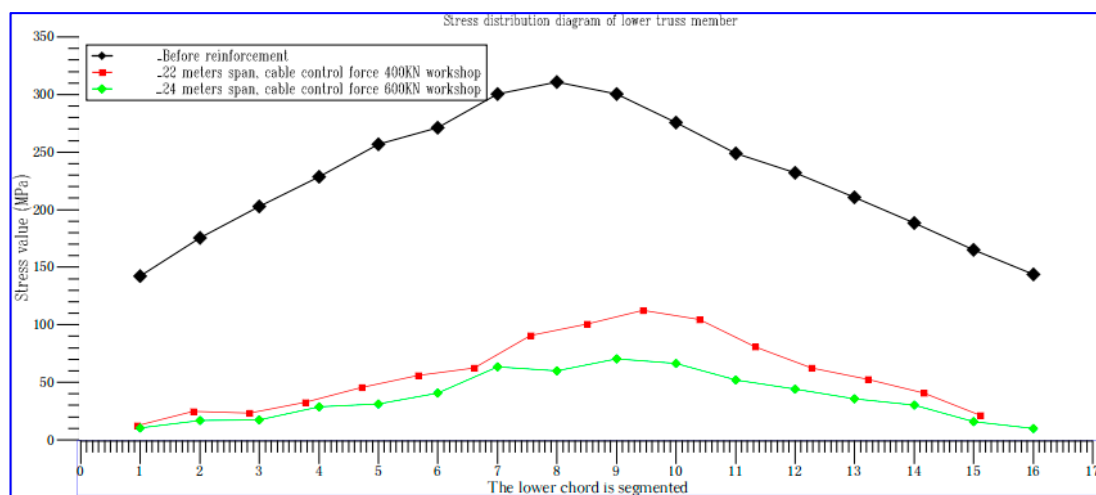


Figure 14. Stress distribution diagram of the lower truss members.

Figure 15 shows that the maximum compressive stress of the upper member of the reinforced front truss exceeded the yield strength of the steel used for the upper member, with the value reaching 155.85 MPa. Some members will be damaged. The compressive stress value of the upper member almost reached 30 MPa, and the stress value was greatly reduced after the reinforcement with a variable axial force cable. When the original truss

was a single-span truss that was a simply supported structure, the mid-span maximum compressive stress of the upper member was nearly three times that of the fulcrum. The multi-point elastic support provided by the reinforced cable reduced the span of a single span, thus decreasing the compressive stress difference of the upper component. This resulted in more uniform stress of the component and increased structural life. Due to the influence of the initial tension of the cable, the truss has an upward arch under the action of a dead load, and there is a reserve of tensile stress on the upper member. When the strain is applied to the whole truss, the reserve stress generated by the initial tension can offset part of the load effect, resulting in a substantial reduction in the tensile stress value.

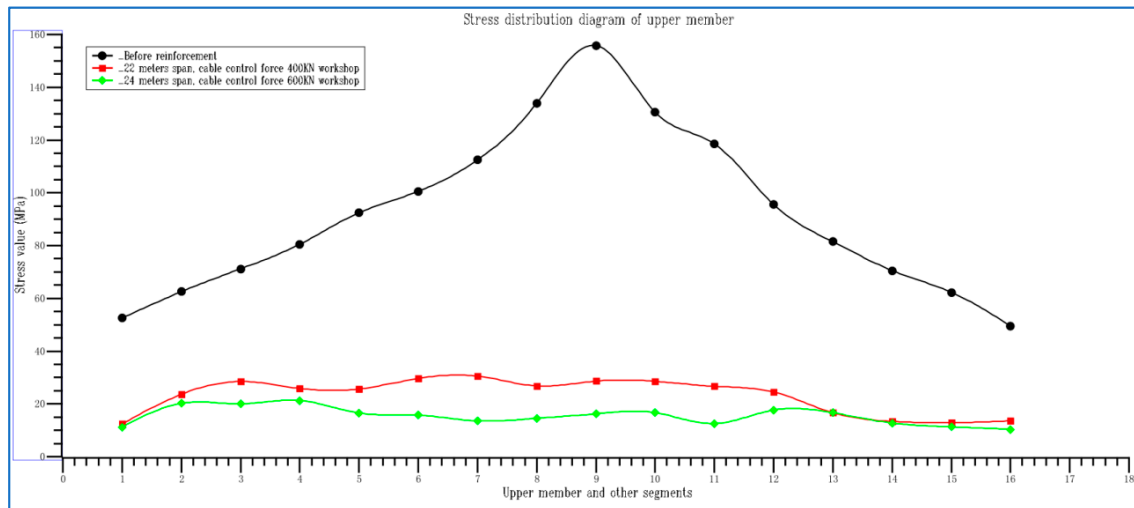


Figure 15. Stress distribution diagram of the upper truss member.

As shown in Figure 16, the stress distribution of the inclined rod of the reinforced front truss consisted of two inclined rods connected to the same node (one under tension and one under pressure), whilst the absolute value of the stress decreased continuously from the fulcrum to the span [30]. After reinforcement, eight of the 24 diagonal rods on each side were placed under tension, whilst 16 were under pressure. Furthermore, the two diagonal rods at the node position of the cable anchorage were under pressure, whilst the tension and pressure of nodes at adjacent positions were placed alternately. The details presented in Table 2 below can also be seen in Figures 16–18.

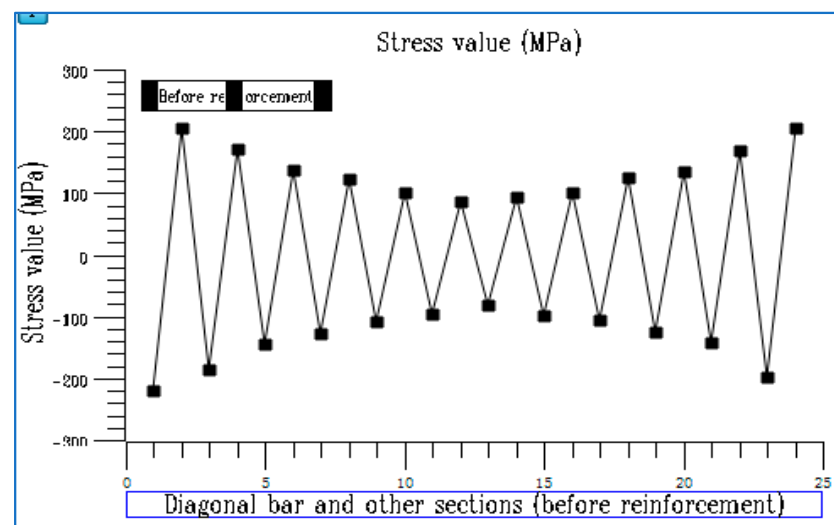
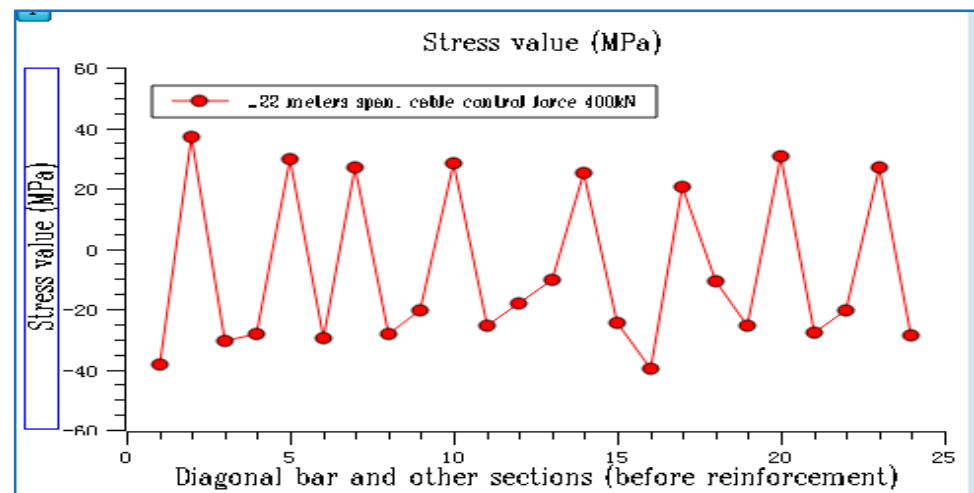
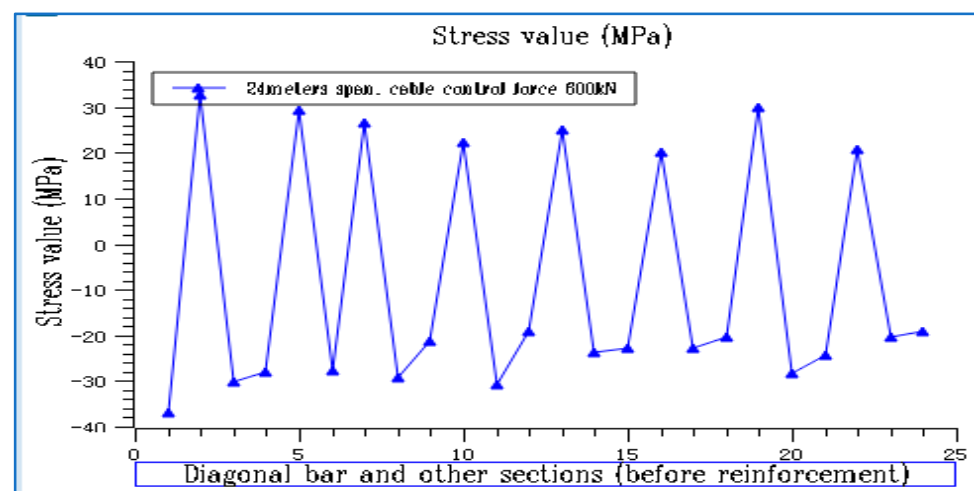


Figure 16. State before reinforcement.

Table 2. The stress changes in the inclined bar of the truss after cable reinforcement.

Component Name	Maximum Compressive Stress (MPa)/Position	Component Name	Maximum Compressive Stress (MPa)/Position	Reduced Value (MPa)
Reinforce the front inclined bar	219/Near-truss	Reinforce the rear diagonal bar	33.8/Near-truss	185.2 ↓
Reinforce the front mid-span diagonal bar	73.5	Reinforce the diagonal bar in the middle of the rear span	38.2	34.6 ↓
The rear inclined rod was reinforced with 22 m controlling force and 400 kN cable	39.9	The rear inclined rod was reinforced with a 24 m controlling force of 600 kN cable	38.2	1.7 ↓

Note: ↓: It means to decrease or decrease.

**Figure 17.** 400 kN control force cable after reinforcement.**Figure 18.** 600 kN control cable after reinforcement.

By comparing the stress changes after the control force changes, the maximum stress value of the inclined bar with a 22 m span and 400 kN control force decreased by 1.7 MPa compared with that with a 24 m span and 600 kN control force. Therefore, the maximum stress value of the inclined bar changes with the span and control force.

By comparing the deflection, stress values of the upper and lower truss members and inclined bar of two kinds of plant trusses with variable axial force reinforcement under live load, the results showed that, in terms of the reinforcement of large-span trusses, the cable with a large controlling force within a reasonable span had better performance, and the controlling force increased with the increase in span. According to the standard, the 600 kN control force can be considered the conventional control force. The cable reinforcement produces a certain inclination angle, and the Z-component increases, which greatly unloads the powerhouse truss. Moreover, the vertical support provided by the cable can transform the large-span simply supported structure into a multi-span continuous structure, thus shortening the span of the single-span structure and greatly reducing its internal force value.

4. Nodal Analysis

4.1. FE Modelling

A solid model was established for the lug plate at the joint position of the plant with complex forces (Figure 19). The joint plate was made of Q345B [30] steel, and the thickness was 20 mm. Each side of the roof truss was provided with internal and external node plates, each with a diameter of 20 mm large hexagonal head high-strength bolts 64 and a hole diameter of 22 mm. The bolt strength class was 10.9 S, and the bolt pretension ranged from 155–187 kN, the value of which was specified in Appendix B of the GB50205-2020 Steel Structure Engineering Construction Quality Acceptance Standard [31].

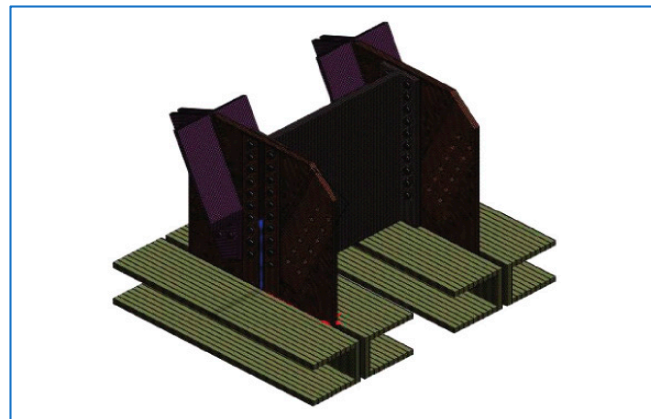


Figure 19. Finite element model of gusset plate.

Here, the force of each member of the node was transferred through welded connections, such as the flange plate and bottom plate, and friction was provided by friction-type high-strength bolts [5]. The ASET software was used to establish the model. The material nonlinearity and geometric linearity were considered in the calculation, and the model was loaded in five steps, according to the GB50344-2004 Technical Standard of Building Structure Inspection, thus ensuring the convergence of the calculation structure. To save computing resources, only bolts were established in this paper (the stress test of side plate materials was omitted). For the simulation test, we selected the most unfavourable joint plate with the greatest internal force before and after reinforcement.

4.2. Node Plate Analysis

As can be seen, the stress value of the bolt group is greatly reduced after adding cable reinforcement, which improves the overall stability of the powerhouse trusses.

5. Conclusions

- (1) After the cable reinforcement, the stiffness of the building truss increased, and the stress distribution trend of each component changed. Under the action of the crane and other main live loads, the reduction rate of the deflection value exceeded 50%. Fur-

thermore, the maximum stress reduction rates of the upper and lower truss members exceeded 60%, whilst the overall load increase rates of the first and second powerhouse trusses exceeded 70% (Figures 11–21) after being reinforced by the variable axial force cable.

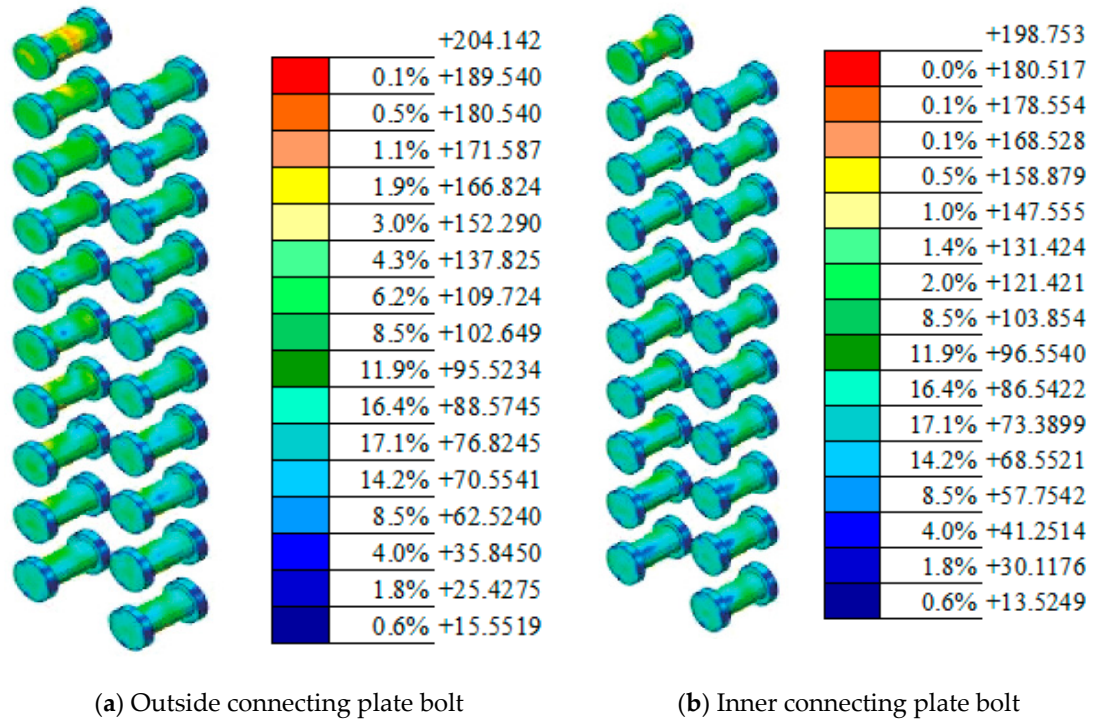


Figure 20. Stress distribution diagram of the bolt before reinforcement.

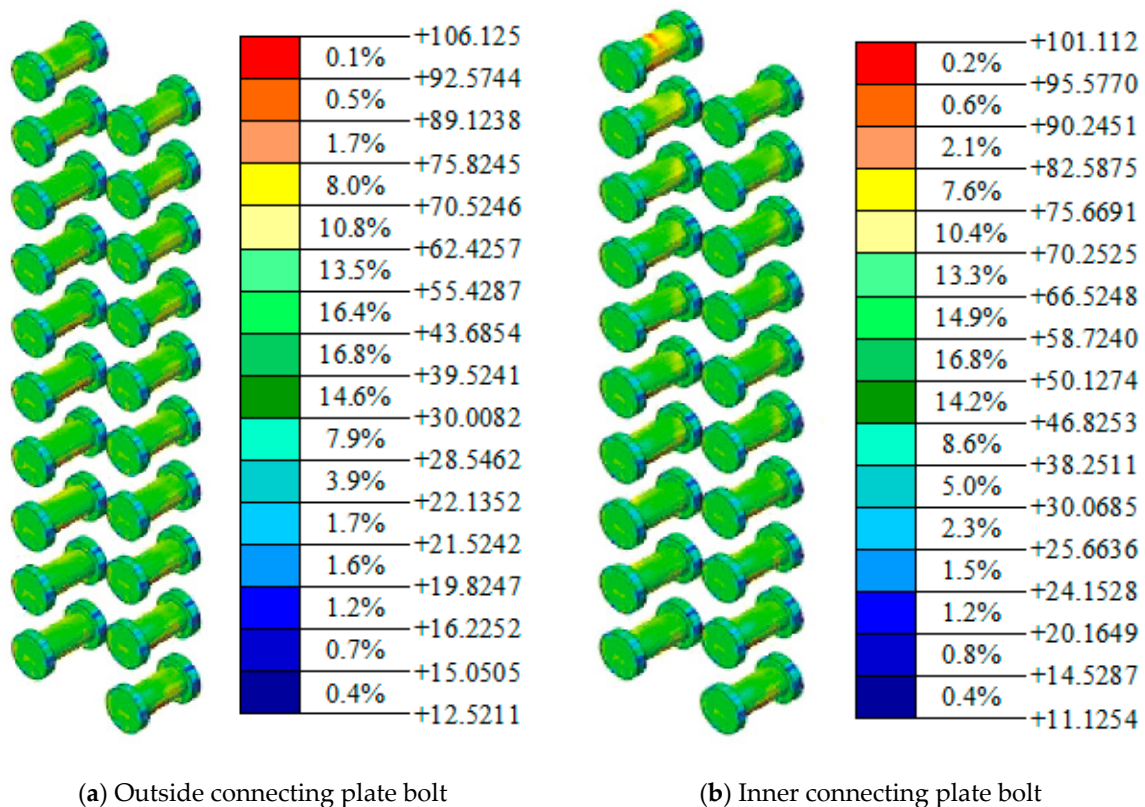


Figure 21. Stress distribution of bolts reinforced with 600 kN cable with 24 m controlling force.

- (2) Before reinforcement, the overall stress level of each node was reasonable, but this increased due to the increased load and service life limit after the installation of photovoltaic panels, along with the second-highest stress concentration at the bolt position of the node plate. After the reinforcement, the stress values of the node plates all decreased significantly. Moreover, the stress below 100 MPa accounted for over 90% of the nodes, whilst the higher stress accounted for less than 1% of the nodes (Tables 1 and 2). The node plates after the reinforcement were in the stable stress area without tearing or stress damage.
- (3) The high-stress and secondary high-stress areas of the bolt group were mainly distributed near the load position. After the reinforcement, the stress zone area of 50–100 MPa accounted for about 35% of the bolt group, whilst the stress zone area above 100 MPa accounted for less than 1% (Table 3) TA. The problem of stress concentration has been solved, and the requirements of the new specification have been met.

Table 3. Results of the comparative analysis of Figure 20a,b and Figure 21a,b.

Condition	Maximum Stress of the Connecting Plate Bolt (MPa)	The Stress Distribution Area above 100 MPa Accounted for (%)	The Stress Distribution Area between 50 and 100 MPa Accounted for (%)	The Stress Distribution Area below 50 MPa Accounted for (%)
Before reinforcement	204	25.6	68.1	6.3
After using 24 m of control force and 600 kN cable reinforcement	106	0.1 ↓	34.6 ↓	65.3 ↑

Note: ↓: It means to decrease or decrease. ↑: It means to rise or increase.

In summary, the plant truss reinforced using the variable axial force cable method can play a role in lifting and strengthening the whole truss [3]. Two kinds of cables with different spans and controlling forces were used to conduct load-lifting reinforcement application practice in Powerhouses 1 and 2. Through comprehensive comparative analysis, the results revealed that the cable reinforcement of powerhouse trusses plays an active and effective role in the stress system. When the cable reinforcement of Powerhouse 2 was used with a 24 m span and controlling force of 600 kN, the reinforcement effect of the structural system was better than that of Powerhouse 1.

Author Contributions: Conceptualization, Z.S. (Zizhen Shen); methodology, Z.S. (Zizhen Shen); software, Z.S. (Zizhen Shen); validation, M.H. and X.L.; formal analysis, X.L.; investigation, L.W.; resources, X.W.; data curation, M.H.; writing—original draft preparation, Z.S. (Zizhen Shen); writing—review and editing, X.L.; visualization, Z.S. (Zizhen Shen); supervision, X.W.; project administration, Z.S. (Zigang Shen); funding acquisition, Z.S. (Zigang Shen). All authors have read and agreed to the published version of the manuscript.

Funding: This research was funded by [Research Project of Zhejiang Provincial Department of Housing and Urban-Rural Development] grant number [2022K010] and The APC was funded by [Zhejiang Provincial Department of Housing and Urban-Rural Development].

Conflicts of Interest: The authors declare no conflict of interest.

References

1. Wang, X.; Yang, Y.; Xin, X.; Jia, J.; Xu, G.; Chen, Z. Computer Aided Design and Numerical Simulation of Dongming Yellow River Bridge Strengthened by a Cable-Stayed System. In Proceedings of the 2021 3rd International Conference on Artificial Intelligence and Advanced Manufacture, Manchester, UK, 23–25 October 2021; pp. 2625–2633.
2. Cai, H.; Aref, A.J. On the design and optimization of hybrid carbon fiber reinforced polymer-steel cable system for cable-stayed bridges. *Compos. Part B Eng.* **2015**, *68*, 146–152. [[CrossRef](#)]
3. Ceballos, M.A.; Prato, C.A. Determination of the axial force on stay cables accounting for their bending stiffness and rotational end restraints by free vibration tests. *J. Sound Vib.* **2008**, *317*, 127–141. [[CrossRef](#)]
4. Simões, L.M.C.; Negrão, J.H.O. Sizing and geometry optimization of cable-stayed bridges. *Comput. Struct.* **1994**, *52*, 309–321. [[CrossRef](#)]
5. Song, C.; Xiao, R.; Sun, B. Optimization of cable pre-tension forces in long-span cable-stayed bridges considering the counterweight. *Eng. Struct.* **2018**, *172*, 919–928. [[CrossRef](#)]

6. Malekinejad, M.; Rahgozar, R. An analytical approach to free vibration analysis of multi-outrigger-belt truss-reinforced tall buildings. *Struct. Des. Tall Spec. Build.* **2013**, *22*, 382–398. [[CrossRef](#)]
7. Khanorkar, A.; Sukhdeve, S.; Denge, S.V.; Raut, S.P. Outrigger and belt truss system for tall building to control deflection: A review. *GRD J. Glob. Res. Dev. J. Eng.* **2016**, *1*, 6–15.
8. Qi, J.; Yang, H.C. Improvement of a truss-reinforced, half-concrete slab floor system for construction sustainability. *Sustainability* **2021**, *13*, 3731. [[CrossRef](#)]
9. Hwang, J.S.; Lee, K.S. Seismic strengthening effects based on pseudodynamic testing of a reinforced concrete building retrofitted with a wire-woven bulk kagome truss damper. *Shock. Vib.* **2016**, *2016*, 1–17. [[CrossRef](#)]
10. American Society of Civil Engineers. *Minimum Design Loads and Associated Criteria for Buildings and Other Structures*; American Society of Civil Engineers: New York, NY, USA, 2017.
11. Hou, Z.; He, W.; Zhou, J.; Qiu, L. national standard «Code for acceptance of construction quality of steel structure engineering» GB50205 Introduction of special research results in revision. *Stand. Eng. Constr.* **2014**, 49–55. [[CrossRef](#)]
12. Keane, B.; Schwarz, G.; Thurnherr, P. Cables and cable glands for hazardous locations. In Proceedings of the 2018 IEEE Petroleum and Chemical Industry Technical Conference (PCIC), Cincinnati, OH, USA, 24–27 September 2018; Volume 42, p. 9.
13. Revanna, N.; Moy, C.K.S.; Krevaiakas, T. *Verifying a Finite Element Analysis Methodology with Reinforced Concrete Beam Experiments*; Research Press of America, Ed.; Research Press of America 2020 Paper Collection IV; Scientific Research Publishing: Chengdu, China, 2021; pp. 340–347.
14. Teng, J.G.; Yu, T.; Fernando, D. Strengthening of steel structures with fiber-reinforced polymer composites. *J. Constr. Steel Res.* **2012**, *78*, 131–143. [[CrossRef](#)]
15. Gardner, L. Stability and design of stainless steel structures—Review and outlook. *Thin-Walled Struct.* **2019**, *141*, 208–216. [[CrossRef](#)]
16. Subramanian, N. *Design of Steel Structures*; Oxford University Press: Oxford, UK, 2008.
17. Trahair, N.S.; Bradford, M.A.; Nethercot, D.A.; Gardner, L. *The Behaviour and Design of Steel Structures to EC3*; CRC Press: Boca Raton, FL, USA, 2017.
18. Ban, H.; Shi, G. A review of research on high-strength steel structures. *Proc. Inst. Civ. Eng. Struct. Build.* **2018**, *171*, 625–641. [[CrossRef](#)]
19. Marshall, J.D.; Jaiswal, K.; Gould, N.; Turner, F.; Lizundia, B.; Barnes, J.C. Post-earthquake building safety inspection: Lessons from the Canterbury, New Zealand, earthquakes. *Earthq. Spectra* **2013**, *29*, 1091–1107. [[CrossRef](#)]
20. Bortolini, R.; Forcada, N. Building inspection system for evaluating the technical performance of existing buildings. *J. Perform. Constr. Facil.* **2018**, *32*, 04018073. [[CrossRef](#)]
21. Ferraz, G.T.; De Brito, J.; De Freitas, V.P.; Silvestre, J.D. State-of-the-art review of building inspection systems. *J. Perform. Constr. Facil.* **2016**, *30*, 04016018. [[CrossRef](#)]
22. Wen, J.; Liu, L.; Jiao, Q.; Yang, J.; Liu, Q.; Chen, L. Failure analysis on 20MnTiB steel high-strength bolts in steel structure. *Eng. Fail. Anal.* **2020**, *118*, 104820. [[CrossRef](#)]
23. Caccese, V.; Mewer, R.; Vel, S.S. Detection of bolt load loss in hybrid composite/metal bolted connections. *Eng. Struct.* **2004**, *26*, 895–906. [[CrossRef](#)]
24. Schauwecker, F.; Moncayo, D.; Middendorf, P. Characterization of high-strength bolts and the numerical representation method for an efficient crash analysis. *Eng. Fail. Anal.* **2022**, *137*, 106249. [[CrossRef](#)]
25. Ahmad, F.; Bajpai, P.K. Evaluation of stiffness in a cellulose fiber reinforced epoxy laminates for structural applications: Experimental and finite element analysis. *Def. Technol.* **2018**, *14*, 278–286. [[CrossRef](#)]
26. Jake, F.; Fidelis, M. Finite Element Analysis of Telecommunication Structure Reinforcement. *ce/papers* **2022**, *5*, 1084–1091. [[CrossRef](#)]
27. Chhushyabaga, B.; Karki, S.; Khadka, S.S. Effect of Mechanical Vibration in a Power House Located in the Nepal Himalaya. In *IOP Conference Series: Earth and Environmental Science*; IOP Publishing: Bristol, UK, 2022; Volume 1037, p. 012065.
28. Kiarasi, F.; Babaei, M.; Sarvi, P.; Asemi, K.; Hosseini, M.; Omid Bidgoli, M. A review on functionally graded porous structures reinforced by graphene platelets. *J. Comput. Appl. Mech.* **2021**, *52*, 731–750.
29. Lin, Y.H.; Lin, Z.H.; Chen, Q.T.; Lei, Y.P.; Fu, H.G. Laser in-situ synthesis of titanium matrix composite coating with TiB–Ti network-like structure reinforcement. *Trans. Nonferrous Met. Soc. China* **2019**, *29*, 1665–1676. [[CrossRef](#)]
30. López, D.L.; Roca, P.; Liew, A.; Echenagucia, T.M.; Van Mele, T.; Block, P. A three-dimensional approach to the Extended Limit Analysis of Reinforced Masonry. In *Structures*; Elsevier: Amsterdam, The Netherlands, 2022; Volume 35, pp. 1062–1077.
31. Koshcheev, A.A.; Roshchina, S.I.; Naichuk, A.Y.; Vatin, N.I. The effect of eccentricity on the strength characteristics of glued rods made of steel cable reinforcement in solid wood. In *IOP Conference Series: Materials Science and Engineering*; IOP Publishing: Bristol, UK, 2020; Volume 896, p. 012059.

Disclaimer/Publisher’s Note: The statements, opinions and data contained in all publications are solely those of the individual author(s) and contributor(s) and not of MDPI and/or the editor(s). MDPI and/or the editor(s) disclaim responsibility for any injury to people or property resulting from any ideas, methods, instructions or products referred to in the content.